

SEARCH FOR PARITY MIXING IN THE  $^{93}\text{Tc } \frac{17}{2}$  ISOMER:  
MEASUREMENTS OF PARTIAL  $\gamma$ -DECAY WIDTHSB. A. BROWN <sup>†</sup>*Cyclotron Laboratory, Michigan State University, East Lansing, Michigan 48824, USA*

and

O. HÄUSSER, T. FAESTERMANN <sup>\*\*</sup>, D. WARD, H. R. ANDREWS and D. HORN <sup>\*\*\*</sup>*Atomic Energy of Canada Limited, Chalk River Nuclear Laboratories, Chalk River, Ontario,  
Canada K0J 1J0*

Received 19 April 1978

**Abstract:** The angular distributions and linear polarizations of  $\gamma$ -rays emitted by the  $\tau = 15 \mu\text{s } \frac{17}{2}^-$  isomer in  $^{93}\text{Tc}$  have been determined. The results imply upper limits of  $\leq 6\%$  for the parity-violating E2 component in the 750.78 keV  $\frac{17}{2}^- \rightarrow \frac{13}{2}^+$  transition and of  $\leq 0.06$  eV for the parity-violating matrix element,  $|\langle \frac{17}{2}^+ | H_{p.v.} | \frac{17}{2}^- \rangle|$ . The  $\frac{17}{2}^- \rightarrow \frac{17}{2}^+$  level spacing was determined to be  $0.30 \pm 0.03$  keV and the corresponding E1 branch was found to be  $\leq 6\%$  of the  $\frac{17}{2}^- \rightarrow \frac{13}{2}^+$  branch.

E NUCLEAR REACTIONS  $^{65}\text{Cu}(^{32}\text{S}, 2n2p)$ ,  $E = 120$  MeV; measured  $\gamma(\theta)$ , linear polarization of delayed  $\gamma$ -rays,  $^{93}\text{Tc}$  deduced levels,  $\gamma$ -branching,  $\delta$ , limit on parity-violating E2 component in  $\frac{17}{2}^- \rightarrow \frac{13}{2}^+$  transition. Enriched target, pulsed beam.

## 1. Introduction

In the last ten years there has been tremendous theoretical progress in the development of unified models for the weak and electromagnetic interactions by Weinberg and others <sup>1)</sup>. The models have successfully predicted the existence of weak neutral currents, but the predicted parity-violating (p.v.) aspects of the weak neutral currents remain to be verified. Measurements of p.v. admixtures in nuclear levels provide a means of testing the purely hadronic part of the weak currents if the complexities associated with the strong interaction can be taken into account <sup>2)</sup>. The situation would be particularly promising if the most important term is associated with charged pion exchange between nucleons; in this case the calculations are relatively straightforward and the existence of p.v. weak neutral currents are predicted to lead to a large enhancement over the calculation with charged currents alone <sup>3)</sup>.

<sup>†</sup> Present address: Nuclear Physics Laboratory, Oxford, England.<sup>\*\*</sup> NRCC Postdoctoral Fellow. Present address: Technische Universität, Munich, W. Germany.<sup>\*\*\*</sup> NRCC Postdoctoral Fellow.

The most definitive experimental evidence for nuclear parity violation comes from the  $\gamma$ -decay of the  $^{180}\text{Hf}$   $8^-$  isomer<sup>4</sup>). However, the theoretical calculation in this case can only be carried out qualitatively<sup>2</sup>). Quantitative calculations can be carried out for the two-nucleon system or for nuclei that can be described by microscopic (e.g., shell model) wave functions such as those in the 2s-1d shell. The results of time-consuming polarized-beam and  $\gamma$ -ray circular-polarization experiments in the nuclei  $^{18}\text{F}$  [ref. 5)] and  $^{19}\text{F}$  [ref. 6)] have recently begun to approach the accuracies required to check the theory.

An interesting case in the intermediate mass region exists in the  $^{93}\text{Tc}$   $\frac{17^-}{2} - \frac{17^+}{2}$  doublet<sup>7,8</sup>). These states can be well described in the shell model, predominantly by  $1g_{7/2} - 2p_{3/2}$  valence configurations. Most importantly, these two states are separated by only 0.3 keV and have partial decay widths to the  $\frac{13^+}{2}$  level which differ by  $2 \times 10^6$ ; hence, the  $\frac{17^-}{2} \rightarrow \frac{13^+}{2}$  decay is extremely sensitive to mixing between these two states. The measured lifetime alone gives an upper limit of about 0.3 eV for the  $\frac{17^-}{2} - \frac{17^+}{2}$  p.v. matrix element<sup>7</sup>). Parity-violating matrix elements are expected to have a size on the order of  $10^{-6}$  of the strong interaction matrix elements (i.e.  $\approx 1$  eV) in favorable cases. Thus the possibility exists that a p.v. interaction can give rise to very large effects in  $^{93}\text{Tc}$ .

We have tried to measure p.v. effects in  $^{93}\text{Tc}$  by carrying out relatively straightforward experiments in which the strength of the E2 component in the  $\frac{17^-}{2} \rightarrow \frac{13^+}{2}$  transition is measured. M2 and E3 decays are allowed if the states have good parity, but the parity mixing allows an "abnormal E2" (denoted by  $\widetilde{\text{E2}}$ ) component. In a previous experiment<sup>8</sup>) an upper limit of 33%  $\widetilde{\text{E2}}$  was established from a measurement of the internal conversion coefficient and it was observed that the limit could be made lower if the E3/M2 mixing ratio could be measured.

In the present experiment, precision measurements of  $\gamma$ -ray angular distributions and linear polarizations have been carried out for the delayed transitions in  $^{93}\text{Tc}$ . From these experiments we have established an upper limit of 6% for the  $\widetilde{\text{E2}}$  strength in the  $\frac{17^-}{2} \rightarrow \frac{13^+}{2}$  transition. The determination of this limit depends on a measurement of the  $(\frac{17^-}{2} \rightarrow \frac{17^+}{2})/(\frac{17^-}{2} \rightarrow \frac{13^+}{2})$  branching ratio for which we obtain an upper limit also of 6%. With this result, the p.v. matrix element between the  $\frac{17^-}{2}$  and  $\frac{17^+}{2}$  levels is found to be  $\leq 0.06$  eV. The E3/M2 mixing ratio from the present work allows one to estimate the  $\widetilde{\text{E2}}$ /M2 interference which might be determined in future experiments by measuring either the  $\gamma$ -ray circular polarization or the  $\gamma$ -asymmetry from polarized nuclei.

The angular-distribution and linear-polarization experiments are described in sects. 2-4. In sect. 5 the results are used to extract decay strengths for the delayed transitions to the  $\frac{13^+}{2}$  level. The  $(\frac{17^-}{2} \rightarrow \frac{17^+}{2})/(\frac{17^-}{2} \rightarrow \frac{13^+}{2})$  branching ratio is discussed in sect. 6 and this is put together with the results obtained in sect. 5 to obtain the  $\frac{17^-}{2} \rightarrow \frac{13^+}{2}$   $\widetilde{\text{E2}}$  strength. The p.v. matrix element is discussed in sect. 7.

## 2. Experimental arrangement

Levels in  $^{93}\text{Tc}$  were populated by the  $^{65}\text{Cu}(^{32}\text{S}, 2p2n)$  reaction at  $E(^{32}\text{S}) = 120$  MeV with the pulsed  $^{32}\text{S}^{10+}$  beam of the Chalk River MP tandem accelerator. The same reaction was recently employed<sup>9)</sup> to measure the  $g$ -factor of the  $\frac{1}{2}^-$  isomer. The large alignment produced by the reaction can be preserved over times comparable to the isomer lifetime (15  $\mu\text{s}$ ) by implanting the long-range recoils into suitable backings such as Pb or Hg [ref. 9)]. In the present work 1.8 mg/cm<sup>2</sup> thick  $^{65}\text{Cu}$  foils were used backed by 64 mg/cm<sup>2</sup> of Pb. The Pb backing was thick enough to stop both recoils and the incident  $^{32}\text{S}$  beam. The target chamber was electrically insulated and had a suppression electrode at a voltage of  $-1.5$  kV at the entrance of the beam to allow precise integration of the beam charge.

The beam was on target for 0.15  $\mu\text{s}$  every 2  $\mu\text{s}$ . Deexcitation  $\gamma$ -rays from isomeric states and from radioactive ground states were observed during a 1.2  $\mu\text{s}$  wide time window which was opened 0.15  $\mu\text{s}$  after the end of each beam pulse. A 15% efficient Ge(Li) detector (A) was placed with its front face 12.2 cm from the target to measure

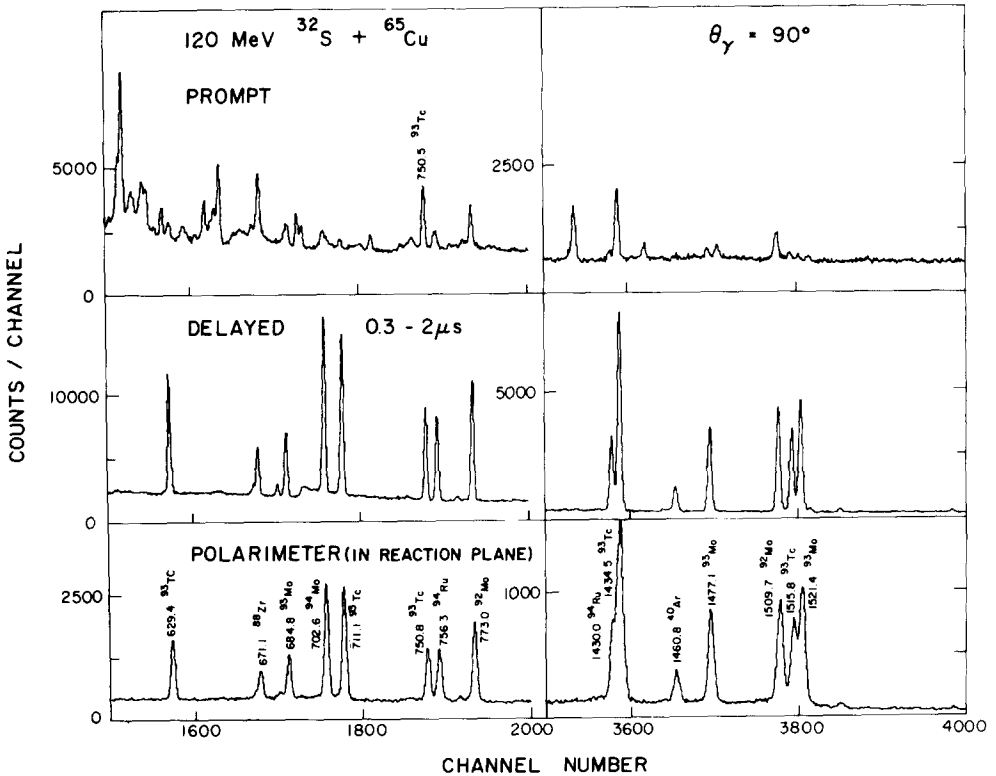


Fig. 1. Comparison of prompt (top) and delayed  $\gamma$ -spectra from the 120 MeV  $^{32}\text{S} + ^{65}\text{Cu}$  reaction. The lower spectrum represents the sum of pulse heights from two of the three detectors making up the three Ge(Li) Compton polarimeter.

the  $\gamma$ -ray angular distributions. Great care was taken to determine the detector angle with respect to the well-collimated beam, and to place the target at the centre of rotation.

A second Ge(Li) detector (C) of nearly equal volume and efficiency was fixed at  $\theta_\gamma = 90^\circ$  at the same distance as detector A to ensure similar counting rates and solid angles for both detectors. Singles events from detector C were used to normalize the angular distribution runs. At the same time C served as the scattering crystal of a three Ge(Li) Compton polarimeter. The side (S;  $\theta_\gamma = 90^\circ$ ,  $\phi_\gamma = 0^\circ$ ) and top (T;  $\theta_\gamma = 90^\circ$ ,  $\phi_\gamma = 90^\circ$ ) detectors of the polarimeter were shielded against  $\gamma$ -rays from the target by  $\geq 7.5$  cm of Pb.

Examples of relevant energy regions of delayed and prompt  $\gamma$ -ray spectra are shown in fig. 1. The top and middle spectra were observed at  $\theta_\gamma = 90^\circ$  with detector A. The lower spectrum represents the sum of pulse heights in detectors C and S, and exhibits therefore somewhat worse energy resolution. It is also apparent that the prompt spectra are considerably more complex than the delayed ones and that, in addition to  $^{93}\text{Tc}$ , a large number of final nuclei are produced, ranging in mass from  $A = 88$  to  $A = 94$ .

### 3. Angular distribution measurements

The angular distributions of delayed  $\gamma$ -rays were observed with detector A between  $0^\circ$  and  $90^\circ$  in  $15^\circ$  steps. The runs were repeated at least once for each angle. For the isomeric  $\gamma$ -rays different runs were normalized to each other by a factor obtained from the integrated beam charge or from the summed intensities of isomeric  $\gamma$ -rays in the fixed detector C. The results from both procedures were in excellent agreement. For  $\gamma$ -rays from the decay of long-lived radioactive nuclei the runs were normalized to the intensity of the *same*  $\gamma$ -ray in detector C.

The deadtimes for detectors A and C were determined by delayed pulses which were triggered by a small fraction ( $10^{-3}$ ) of the total counting rate and inserted below the lowest threshold in the  $\gamma$ -ray spectra. The counting losses were generally kept below 20%. Additional deadtimes arise for isomeric  $\gamma$ -rays which may not be counted because one of the preceding prompt  $\gamma$ -rays of high multiplicity  $M_p$  may be registered in the same detector. A complex correction results which depends on the average angular correlations of the  $M_p$   $\gamma$ -rays, on the average total detection efficiency and on the ratio of the isomer lifetime to the pulse-pair resolving time of the counting system. The correction was calculated by making use of results from systematic studies of  $\gamma$ -ray multiplicities in Er and Yb nuclei<sup>10,11</sup>). The correction is not very important for the  $^{93}\text{Tc}$  isomer since it amounts to at most 3% at  $0^\circ$  and to a difference of  $< 1\%$  between  $0^\circ$  and  $90^\circ$ .

A further complication arose in the analysis of the angular distributions because of the existence of a weak static magnetic field of 0.14 mT perpendicular (within  $\pm 5^\circ$ ) to the beam-detector plane which was discovered towards the end of the experiment.

The spins of the isomeric nuclei experience a Larmor precession which amounts, on the average, to an angle  $|\omega\tau| = 7^\circ$  for the  $15 \mu\text{s } \frac{17}{2}^-$  state in  $^{93}\text{Tc}$  ( $g = 1.231 \pm 0.006$ , see ref. <sup>9</sup>). We denote the  $\gamma$ -ray angular distribution at time  $t = 0$  by

$$W(t = 0) = \sum_k a_k P_k(\cos \theta) = \sum_k b_k \cos(k\theta) = \sum_k \left( \sum_{l=k}^{k_{\max}} b_{kl} a_l \right) \cos(k\theta),$$

where

$$b_0 = a_0 + \frac{1}{4}a_2 + \frac{9}{64}a_4 + \frac{50}{512}a_6,$$

$$b_2 = \frac{3}{4}a_2 + \frac{5}{16}a_4 + \frac{105}{512}a_6,$$

$$b_4 = \frac{35}{64}a_4 + \frac{63}{256}a_6,$$

$$b_6 = \frac{231}{512}a_6,$$

The  $a_k$  coefficients are expected to decrease with time because of relaxation processes such as spin-lattice relaxation <sup>12</sup>); we assume here  $a_k(t) = a_k(t = 0) \exp(-t/\tau_k)$ .

The time-integrated angular distributions are then

$$\bar{W} = \sum_{kl} I_{kl} a_l,$$

where

$$\begin{aligned} I_{kl} &= \int_0^\infty \cos k(\theta - \omega t) e^{-t/\tau_l} e^{-t/\tau} dt \\ &= \frac{b_{kl}\tau}{\sqrt{(1 + \tau/\tau_l)^2 + (k\omega\tau)^2}} \cos k(\theta - \Delta'_{kl}), \end{aligned}$$

with

$$\tan k\Delta'_{kl} = \frac{k\omega\tau}{1 + \tau/\tau_l}.$$

Each angular distribution is thus specified by the initial distribution coefficients  $a_l$ , the corresponding relaxation times  $\tau_l$ , and the Larmor precession angle  $\omega\tau$ . After assuming a set of relaxation times the  $a_l$  coefficients have been fitted to the measured distributions (see table 1). The relaxation times for  $^{94}\text{Ru}$  ( $\tau_2 = 76 \mu\text{s}$ ,  $\tau_4 = 24 \mu\text{s}$ ) and for  $^{93}\text{Tc}$  isomers ( $\tau_2 = 85 \mu\text{s}$ ,  $\tau_4 = 45 \mu\text{s}$ ) are in agreement with previous measurements. They represent spin-lattice relaxation times corresponding <sup>12</sup>) to a Knight shift of  $\approx 1\%$ . The extracted  $a_l$  values for  $^{93}\text{Tc}$  (see table 1) are not very sensitive to the choice of  $\tau_l$  because  $\tau_l \gg \tau$ . It will be shown in sect. 5 that the composition of transitions of mixed multipolarity in  $^{93}\text{Tc}$  can be determined independently of  $\tau_l$  by making use of angular distributions of other transitions of unique multipolarity originating from the same isomer.

TABLE 1  
Angular distribution coefficients and linear polarization of anisotropic  $\gamma$ -transitions

Nucleus	$T_{1/2}$ ( $\mu$ s)	$E_\gamma$ (keV)	$J_i^\pi \rightarrow J_f^\pi$	$M\lambda$	$a_2(t=0)^a$	$a_4(t=0)^a$	$P_{\text{exp}}$	$P_{\text{calc}}^a$
$^{93}\text{Tc}$	$10.1 \pm 0.3$	629.44	$\frac{1}{2}^- \rightarrow \frac{1}{2}^+$	E1	$-0.185 \pm 0.008$	$0.019 \pm 0.014$	$0.231 \pm 0.033$	$0.215 \pm 0.010$
		711.11	$\frac{3}{2}^- \rightarrow \frac{3}{2}^+$	E1	$0.312 \pm 0.006$	$0.002 \pm 0.010$	$-0.479 \pm 0.031$	$-0.453 \pm 0.010$
		750.78	$\frac{1}{2}^- \rightarrow \frac{1}{2}^+$	$\tilde{\text{E}}2/\text{M}2/\text{E}3$	$-0.191 \pm 0.008$	$-0.262 \pm 0.013$	$0.233 \pm 0.041$	see text
		1434.52	$\frac{1}{2}^+ \rightarrow \frac{1}{2}^+$	E2	$0.247 \pm 0.006$	$-0.043 \pm 0.010$	$0.372 \pm 0.054$	$0.327 \pm 0.013$
		1516.0	$\frac{1}{2}^+ \rightarrow \frac{3}{2}^+$	M1/E2	$-0.086 \pm 0.011^b$	$0.155 \pm 0.017^b$	$0.089 \pm 0.081^b$	$0.075 \pm 0.010$
$^{93}\text{Ru}$	$2.05 \pm 0.10$	544.65	$\frac{1}{2}^+ \rightarrow \frac{1}{2}^+$	E2	$0.220 \pm 0.007$	$-0.046 \pm 0.046$	$0.356 \pm 0.045$	$0.345 \pm 0.011$
		1392.25	$\frac{1}{2}^+ \rightarrow \frac{3}{2}^+$	E2	$0.246 \pm 0.009$	$-0.036 \pm 0.012$	$0.411 \pm 0.097$	$0.401 \pm 0.015$
$^{90}\text{Mo}$	$1.14 \pm 0.05$	809.56	$6^+ \rightarrow 4^+$	E2	$0.180 \pm 0.006$	$-0.039 \pm 0.007$	$0.312 \pm 0.035$	$0.274 \pm 0.009$
		947.98	$2^+ \rightarrow 0^+$	E2	$0.184 \pm 0.005$	$-0.030 \pm 0.007$	$0.282 \pm 0.040$	$0.287 \pm 0.008$
		1054.2	$4^+ \rightarrow 2^+$	E2	$0.180 \pm 0.006$	$-0.031 \pm 0.008$	$0.310 \pm 0.068$	$0.279 \pm 0.009$
$^{94}\text{Ru}$	$68 \pm 10$	311.77	$6^+ \rightarrow 4^+$	E2	$0.143 \pm 0.019$	$0.034 \pm 0.055$	$-0.005 \pm 0.042$	$0.076 \pm 0.040$
		756.23	$4^+ \rightarrow 2^+$	E2	$0.167 \pm 0.028$	$0.037 \pm 0.083$	$0.115 \pm 0.044$	$0.089 \pm 0.035$
		1429.96	$2^+ \rightarrow 0^+$	E2	$0.183 \pm 0.028$	$-0.056 \pm 0.080$	$0.028 \pm 0.087$	$0.098 \pm 0.035$

<sup>a)</sup> For the long-lived isomers in  $^{93}\text{Tc}$  and  $^{94}\text{Ru}$ , the results depend on the assumed spin-relaxation times,  $\tau_2 = 85 \mu\text{s}$  and  $\tau_4 = 45 \mu\text{s}$  for  $^{93}\text{Tc}$ , and  $\tau_2 = 76 \mu\text{s}$  and  $\tau_4 = 24 \mu\text{s}$  for  $^{94}\text{Ru}$  (see ref. <sup>9)</sup>). The calculated linear polarizations,  $P_{\text{calc}}$ , deduced mixing ratios and partial  $\gamma$ -decay widths are quite insensitive to this choice.

<sup>b)</sup> These results imply  $\delta(\text{E}2/\text{M}1) = 16.6^{+2.9}_{-2.1}$  for the 1516.0 keV transition.

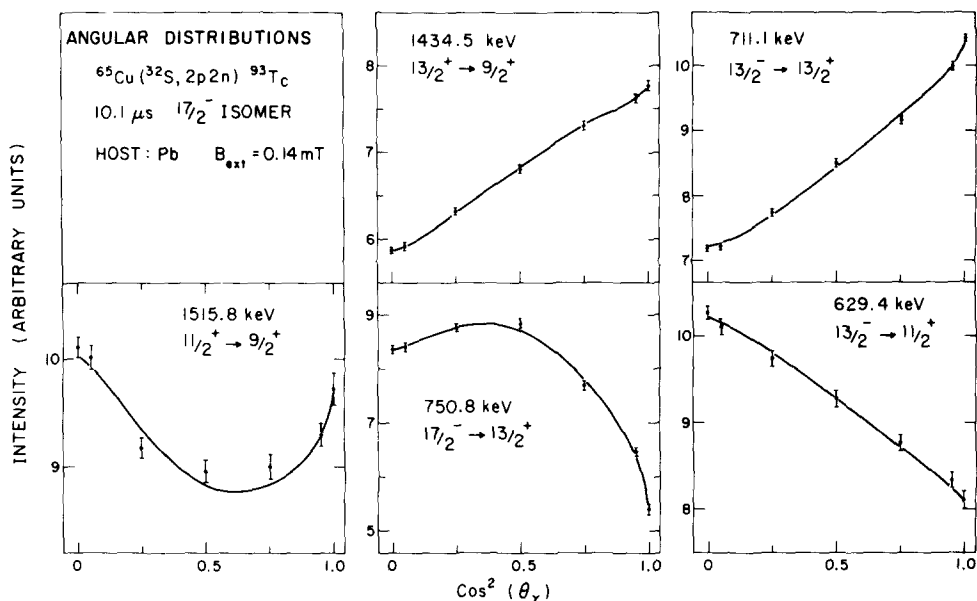


Fig. 2. Angular distributions of  $\gamma$ -rays from the decay of the  $\frac{1}{2}^-$  isomer in  $^{93}\text{Tc}$  ( $T_{1/2} = 10.1 \mu\text{s}$ ). The fitted curves include the integral effect of a precession of  $7^\circ$  for the  $\frac{1}{2}^-$  spin.

TABLE 2

Angular distribution coefficients and linear polarization of nearly isotropic  $\gamma$ -transitions

Nucleus	$E_\gamma$ (keV)	$J_i^\pi \rightarrow J_f^\pi$	$M\lambda$	$a_2(t=0)^a$	$a_4(t=0)^a$	$P_{\text{exp}}^a$	$P_{\text{calc}}^a$
$^{94}\text{Tc}$	367.07	$1^+ \rightarrow (2^+)$	M1/E2	$0.001 \pm 0.008$	$0.016 \pm 0.010$	$0.002 \pm 0.036$	0
$^{94}\text{Mo}$	702.64	$4^+ \rightarrow 2^+$	E2	$0.005 \pm 0.009$	$0.007 \pm 0.012$	$0.017 \pm 0.026$	0
	849.72	$6^+ \rightarrow 4^+$	E2	$-0.008 \pm 0.007$	$0.010 \pm 0.008$	$-0.025 \pm 0.034$	0
	871.09	$2^+ \rightarrow 0^+$	E2	$-0.003 \pm 0.005$	$0.007 \pm 0.006$	$0.020 \pm 0.026$	0
$^{93}\text{Mo}$	684.76	$\frac{1}{2}^+ \rightarrow \frac{3}{2}^+$	E2	$0.003 \pm 0.008$	$0.002 \pm 0.009$	$0.039 \pm 0.050$	0
	1363.00	$\frac{7}{2}^+ \rightarrow \frac{5}{2}^+$	M1/E2	$-0.001 \pm 0.005$	$0.000 \pm 0.006$	$0.005 \pm 0.046$	0
	1477.2	$\frac{9}{2}^+ \rightarrow \frac{5}{2}^+$	E2	$-0.001 \pm 0.010$	$-0.003 \pm 0.013$	$-0.033 \pm 0.072$	0
	1521.4	$\frac{7}{2}^+ \rightarrow \frac{5}{2}^+$	M1/E2	$-0.002 \pm 0.009$	$-0.005 \pm 0.012$	$0.036 \pm 0.068$	0
$^{92}\text{Mo}^a$	329.80	$6^+ \rightarrow 4^+$	E2	$0.025 \pm 0.006$	$-0.004 \pm 0.008$	$0.033 \pm 0.031$	$0.035 \pm 0.009$
	772.97	$4^+ \rightarrow 2^+$	E2	$0.039 \pm 0.009$	$-0.002 \pm 0.011$	$0.024 \pm 0.033$	$0.061 \pm 0.014$
	1509.68	$2^+ \rightarrow 0^+$	E2	$0.014 \pm 0.011$	$-0.005 \pm 0.014$	$-0.010 \pm 0.069$	$0.018 \pm 0.014$
$^{90}\text{Zr}$	1129.14	$6^+ \rightarrow 5^-$	E1	$-0.001 \pm 0.009$	$0.004 \pm 0.011$	$0.017 \pm 0.057$	0

<sup>a</sup>) The weak angular distributions and polarizations observed in  $^{92}\text{Mo}$  arise from population of the well-known 188 ns  $8^+$  isomer <sup>b</sup>) in addition to the strong isotropic components from the decay of 4.4 h  $^{92}\text{Tc}$ .

The fitted  $a_2$  and  $a_4$  coefficients of non-isotropic transitions are shown in table 1. The  $a_k$  coefficients still contain correction factors  $Q_k$ , resulting from the finite size of detector  $A$ . From the carefully measured detector geometry we calculate  $Q_2 = 0.973$  and  $Q_4 = 0.91$  for  $0.4 \text{ MeV} < E_\gamma < 1.5 \text{ MeV}$ . All transitions gave a vanishing  $a_6$  term. The angular distributions of transitions in  $^{93}\text{Tc}$  are shown in fig. 2 with  $\cos^2\theta$  as the ordinate. As a result of the spin precession in the external magnetic field the distributions of transitions with essentially vanishing  $a_4$  coefficient (the 629.4 keV  $\frac{1}{2}^{\text{--}} \rightarrow \frac{1}{2}^{\text{+}}$  E1 transition and the 711.1 keV  $\frac{1}{2}^{\text{--}} \rightarrow \frac{1}{2}^{\text{+}}$  E1 transition) do not follow a straight line.

The  $a_i$  coefficients for  $\gamma$ -rays populated by the decay of radioactive nuclei are shown in table 2. With the exception of the  $^{92}\text{Mo}$   $\gamma$ -rays, which are partially fed by a 188 ns  $8^+$  isomer, the distributions are isotropic to a high degree of accuracy.

All  $\chi^2$  values obtained were close to the expectation value indicating that the procedures described in sect. 2 were carefully followed.

#### 4. Linear polarization measurements

The linear polarization of delayed  $\gamma$ -rays was measured with a three Ge(Li) Compton polarimeter. Its polarization sensitivity arises from the dependence of the Compton scattering cross section on the angle between the plane of polarization of the incident  $\gamma$ -ray and the scattering plane. A polarimeter similar to ours has been described by Butler *et al.*<sup>13)</sup>. The pulse heights for coincident events between the scatterer C and either of the detectors in (S) or perpendicular to (T) the plane of beam and primary radiation were recorded event by event on magnetic tape. On playback of the tapes a quantity was calculated from the pulse-height pairs which equals  $\cos \xi$  for single Compton scattering events. Only events with a scattering angle  $\xi$  in the range allowed by the detector geometry were accumulated in the sum spectra. This requirement improves the peak-to-background ratio by nearly a factor of two because background events from electron escape in the scatterer and of  $\gamma$ -escape in the absorber are removed. It also slightly increases the polarization sensitivity because a fraction of the peak events arising from multiple scattering are eliminated.

From the intensities of  $\gamma$ -rays scattered in the plane of beam and the primary radiation,  $N_{\parallel}$ , and of those scattered perpendicular to it,  $N_{\perp}$ , an asymmetry ratio  $A$  was formed,

$$A = \frac{a(E_\gamma)N_{\perp} - N_{\parallel}}{a(E_\gamma)N_{\perp} + N_{\parallel}},$$

where  $a(E_\gamma)$  is the energy-dependent ratio of detection efficiencies for the two absorber detectors S and T. The asymmetry  $A$  is proportional to the linear polarization  $P(\theta)$  of the primary  $\gamma$  ray, i.e.

$$P(\theta) = \frac{I(\theta, \psi = 0^\circ) - I(\theta, \psi = 90^\circ)}{I(\theta, \psi = 0^\circ) + I(\theta, \psi = 90^\circ)},$$



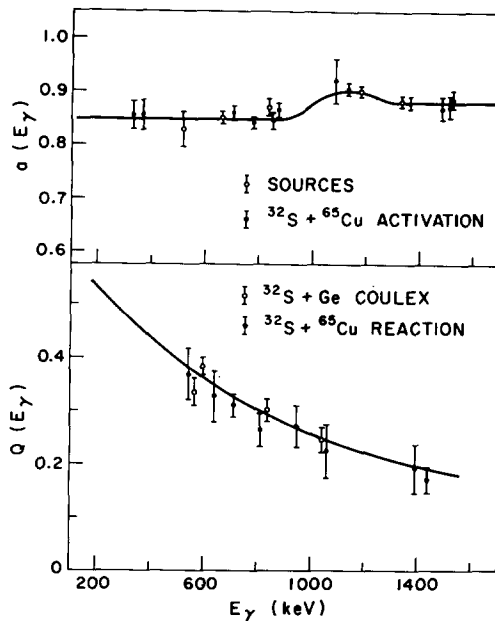


Fig. 3. The asymmetry  $a(E_\gamma)$  and polarization sensitivity  $Q(E_\gamma)$  for the three Ge(Li) Compton polarimeter. The fit to  $Q(E_\gamma)$  (solid line) is explained in the text, whereas the line connecting the measured  $a(E_\gamma)$  was drawn to guide the eye.

TABLE 3  
Coulomb excitation of Ge isotopes with 80 MeV  $^{32}\text{S}$

Isotope	$E_\gamma$ (keV)	$a_2^{\text{exp}}$	$a_2^{\text{calc } a)}$	$a_4^{\text{exp}}$	$a_4^{\text{calc } a)}$	$P_{\text{exp}}^b)$	$P_{\text{calc}}^a)$
$^{70}\text{Ge}$	1040	$0.287 \pm 0.024$	0.271	$-0.038 \pm 0.036$	-0.045	$0.453 \pm 0.040$	0.446
$^{72}\text{Ge}$	835	$0.265 \pm 0.008$	0.245	$-0.044 \pm 0.012$	-0.027	$0.390 \pm 0.024$	0.405
$^{74}\text{Ge}$	596	$0.201 \pm 0.004$	0.208	$0.001 \pm 0.006$	-0.007	$0.326 \pm 0.014$	0.345
$^{76}\text{Ge}$	563	$0.198 \pm 0.005$	0.201	$0.003 \pm 0.007$	-0.004	$0.373 \pm 0.027$	0.335

<sup>a)</sup> Evaluated for thick target using first-order perturbation theory.

<sup>b)</sup> Derived from the polarimeter asymmetry and sensitivity shown in fig. 3.

where  $\theta$  is the angle of the primary  $\gamma$ -ray to the beam and  $I(\theta, \psi)$  is the intensity of  $\gamma$ -rays with their electric vector at an angle  $\psi$  to the plane containing beam and primary  $\gamma$ -ray. We then define

$$A = Q(E_\gamma)P(\theta)$$

where  $Q(E_\gamma)$  is the energy dependent polarization sensitivity of the apparatus.

The efficiency ratio  $a(E_\gamma)$  was determined by using the isotropic  $\gamma$ -rays produced in the  $^{32}\text{S} + ^{65}\text{Cu}$  reaction, and in addition, by radioactive sources of  $^{85}\text{Sr}$ ,  $^{137}\text{Cs}$ ,

<sup>54</sup>Mn and <sup>60</sup>Co, placed at the target position. The results are shown in the upper half of fig. 3. The origin of the bump near 1.1 MeV was not investigated further since the <sup>93</sup>Tc  $\gamma$ -rays of interest are either substantially lower or higher in energy.

The polarization sensitivity  $Q(E_\gamma)$  was calibrated with  $\gamma$ -rays emitted after Coulomb excitation of a thick, natural Ge target with 80 MeV <sup>32</sup>S. The measured angular distribution coefficients of  $2^+ \rightarrow 0^+$  transitions in four even- $A$  Ge isotopes are shown in table 3; they agree well with values calculated in first-order Coulomb excitation theory <sup>14</sup>). The asymmetries measured for the four E2  $\gamma$ -transitions were then fitted to the polarization  $P(\theta)$  calculated from the measured  $a_2$  and  $a_4$  values (see table 3) by

$$A = 0.59Q'(E_\gamma)P(\theta),$$

where

$$Q'(E_\gamma) = (1 + \alpha)/(1 + \alpha + \alpha^2), \quad \text{with } \alpha = E_\gamma/m_0c^2,$$

is the calculated polarization sensitivity for point scatterer and point absorbers. The fitted polarization sensitivity  $Q(E_\gamma)$  is shown in fig. 3 together with experimental points from the Ge calibration and from the reaction  $\gamma$ -rays of table 1 exhibiting a unique multipolarity. The data points closely follow the assumed polarization sensitivity as was already shown by Butler *et al.* <sup>13</sup>).

The linear polarizations of reaction  $\gamma$ -rays were deduced from the measured asymmetries using the fitted polarization sensitivity  $Q(E_\gamma) = 0.59 Q'(E_\gamma)$  shown in fig. 3, and are summarized in tables 1 and 2.

### 5. Evaluation of partial decay widths for the 750.8 keV $\frac{1}{2}^- \rightarrow \frac{1}{2}^+$ transition

The angular distribution coefficients  $a_2$  and  $a_4$  and the measured linear polarization  $P_{\text{exp}}$  for  $\gamma$ -rays originating from the  $\frac{1}{2}^-$  isomer (see table 1) can now be used to extract the partial decay widths contributing to the 750.8 keV  $\frac{1}{2}^- \rightarrow \frac{1}{2}^+$   $\gamma$ -transition. We use here the phase convention of Rose and Brink <sup>15</sup>) and the formulation of the  $\gamma$ -ray linear polarization by Taras <sup>16</sup>).

The angular distribution coefficients for the  $\frac{1}{2}^- \rightarrow \frac{1}{2}^+$  transitions are then

$$a_2 = x_2(0.4202((\tilde{E}2)^2 + (M2)^2 - 1.3004(M2)(E3) + 0.2322(E3)^2),$$

$$a_4 = x_4(-0.1843((\tilde{E}2)^2 + (M2)^2 - 1.4305(M2)(E3) - 0.1130(E3)^2),$$

$$a_6 = x_6(0.4287(E3)^2),$$

where

$$(EL) = \frac{\langle \frac{1}{2}^- || T_L || \frac{1}{2}^+ \rangle}{\sqrt{2L+1}} \Big/ \sqrt{\Gamma}$$

are the square roots of the fractions of the total decay width  $\Gamma$ . The attenuation coefficients  $x_k \leq 1$  take the populations of substates with  $|m| > \frac{1}{2}$  into account and contain

in addition geometrical attenuation coefficients. The  $k = 6$  terms need not be considered since the measured  $a_6 = 0.002 \pm 0.022$  is essentially vanishing. The  $x_2$  coefficient was obtained from the 629.4 keV E1, the 711.1 keV E1 and the 1434.5 keV E2 transitions. The corresponding three  $a_2$  coefficients of table 1 can be fitted by  $x_2 = 0.651 \pm 0.010$ . Similarly, the  $x_4$  coefficient was obtained from the sizeable  $a_4$  coefficients of the 1434.5 keV E2 and of the E2/M1 1516 keV transition, whose mixing ratio is uniquely determined to be  $\delta = 16.6_{-2.1}^{+2.9}$  from the observed  $a_2/x_2$  coefficient. We then obtain  $x_4 = 0.336 \pm 0.034$ . It should be emphasized that, although the values of  $a_k$  and  $x_k$  depend on the assumed relaxation times  $\tau_k$ , the ratio  $a_k/x_k$  is extremely insensitive to the choice of  $\tau_k$  since both the mixed 750.8 keV and the normalizing transitions of pure multipolarity are effected in a similar way. For example, an increase in  $\tau_2$  from 85  $\mu\text{s}$  to 185  $\mu\text{s}$  changed the ratio  $a_2/x_2 = 0.293 \pm 0.014$  by about 1 %.

The experimental values for  $a_2/x_2$  and  $a_4/x_4$  are shown in fig. 4 together with values allowed for a mixed  $\widetilde{\text{E}}2/\text{M}2/\text{E}3 \frac{17}{2}^- \rightarrow \frac{13}{2}^+$  transition. Based on the experimental  $a_2/x_2$  value ( $\widetilde{\text{E}}2$ )<sup>2</sup> values larger than 0.1 can clearly be ruled out.

Let us consider now the linear polarization  $P$  [ref. <sup>16</sup>)] for the  $\frac{17}{2}^- \rightarrow \frac{13}{2}^+$  transition,

$$P = \{ \overline{P}_2^{(2)} x_2 (0.4204 (\widetilde{\text{E}}2)^2 - (\text{M}2)^2) + 0.6502 (\text{M}2) (\text{E}3) + 0.1548 (\text{E}3)^2 \\ + \overline{P}_4^{(2)} x_4 (0.0307 ((\widetilde{\text{E}}2)^2 - (\text{M}2)^2) + 0.0477 (\text{M}2) (\text{E}3) - 0.0753 (\text{E}3)^2) \} \\ \times (2 + 2a_2 \overline{P}_2 + 2a_4 \overline{P}_4)^{-1},$$

where the  $\overline{P}_k$  and  $\overline{P}_k^{(2)}$  are values of (associated) Legendre polynomials, time-averaged over the spin precession angle of the isomer, i.e.  $\overline{P}_2 = -0.400$ ,  $\overline{P}_4 = 0.239$ ,  $\overline{P}_2^{(2)} = 2.508$  and  $\overline{P}_4^{(2)} = -4.915$ . We have then evaluated the multiplicities of the  $\frac{17}{2}^- \rightarrow \frac{13}{2}^+$  transition by calculating  $\chi^2$  for  $a_2/x_2$ ,  $a_4/x_4$  and  $P$  for possible combinations of  $\widetilde{\text{E}}2$ , M2 and E3. The following results have been obtained (errors quoted are one standard deviation):

$$\Gamma(\widetilde{\text{E}}2)/\Gamma = 0.032 \pm 0.032, \quad \Gamma(\widetilde{\text{E}}2) = (3.6 \pm 3.6) \times 10^{-13} \text{ eV}, \\ \Gamma(\text{M}2)/\Gamma = 0.35 \pm 0.10, \quad \Gamma(\text{M}2) = (4.0 \pm 1.2) \times 10^{-12} \text{ eV}, \\ \Gamma(\text{E}3)/\Gamma = 0.62 \pm 0.10, \quad \Gamma(\text{E}3) = (7.1 \pm 1.3) \times 10^{-12} \text{ eV}, \\ \delta(\text{E}3/\text{M}2) = 1.33_{-0.16}^{+0.36}.$$

The 95 % confidence limit on the parity-forbidden width was determined to be  $\Gamma(\text{E}2)/\Gamma < 0.08$ . The widths are most strongly determined by the accurately known  $a_2/x_2$  value, and least strongly by the rather inaccurate  $a_4/x_4$  (see fig. 4). The solution obtained is not significantly altered if the recently measured K-conversion coefficient for the 750.8 keV transition <sup>8</sup>) is included in the fitting procedure, i.e.

$$10^3 \alpha_K = 1.45 (\widetilde{\text{E}}2)^2 + 3.92 (\text{M}2)^2 + 3.36 (\text{E}3)^2 = 3.3 \pm 0.2.$$

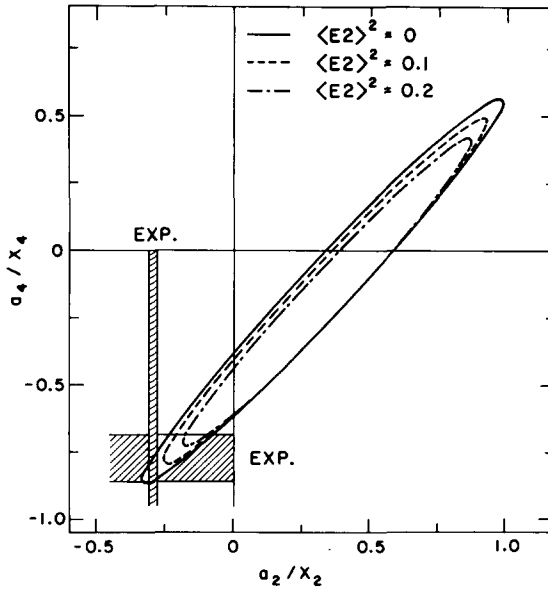


Fig. 4. Possible values of the angular distribution coefficients  $a_2/x_2$  and  $a_4/x_4$  for different E2 components in the  $\frac{1}{2}^- \rightarrow \frac{1}{2}^+$  transition. The experimental values are shown as shaded areas.

The best solution is in close agreement with all known data for the  $\frac{1}{2}^- \rightarrow \frac{1}{2}^+$  transition (measured quantities in brackets):

$$a_2/x_2 = 0.301(0.293 \pm 0.014),$$

$$a_4/x_4 = -0.752(-0.78 \pm 0.09),$$

$$P = 0.240(0.233 \pm 0.041),$$

$$10^3 \alpha_K = 3.50(3.3 \pm 0.2).$$

### 6. Upper limit on the 0.3 keV $\frac{1}{2}^- \rightarrow \frac{1}{2}^+$ E1 branch

The  $\widetilde{E}2$  component in the 750.8 keV transition, estimated in the previous section, has so far been tacitly assumed to result from a parity-violating admixture in the  $\frac{1}{2}^-$  state. However, an E2 transition of slightly lower energy could arise from a  $\frac{1}{2}^- \rightarrow \frac{1}{2}^+ \rightarrow \frac{1}{2}^+$  branch. Since the  $\frac{1}{2}^+$  state is only about 0.3 keV below the  $\frac{1}{2}^-$  isomer<sup>7,8</sup>) a  $\frac{1}{2}^+ \rightarrow \frac{1}{2}^+$  E2 transition of  $\approx 750.5$  keV would result which cannot be resolved in the Ge(Li) detectors from the 750.8 keV transition. The upper limit on the E2 component of the  $\approx 750.8$  keV  $\gamma$ -ray applies therefore to the combined intensities of the  $\frac{1}{2}^- \rightarrow \frac{1}{2}^+ \rightarrow \frac{1}{2}^+$  branch and a genuine parity-violating  $\frac{1}{2}^- \rightarrow \frac{1}{2}^+$   $\widetilde{E}2$  component.

We have derived an upper limit on the E1 branch making use of the very different angular distributions of the  $\frac{17}{2}^- \rightarrow \frac{13}{2}^+$  transition ( $a_2 = -0.191$ ,  $a_4 = -0.262$ ) and of the  $\frac{17}{2}^+ \rightarrow \frac{13}{2}^+$  E2 transition ( $a_2 = +0.24$ ,  $a_4 = -0.05$ ). The relative intensities of both components vary differently with detection angle and the angular variation of the combined centroid is thus characteristic of the branching ratio.

The energy separation  $\Delta$  of the  $\frac{17}{2}^-$  and  $\frac{17}{2}^+$  states was redetermined by comparing the energy shift of the  $\gamma$ -ray peaks at  $\approx 751$  keV in both prompt and delayed spectra (see fig. 1). The prompt  $\frac{17}{2}^- \rightarrow \frac{13}{2}^+$  transition exhibits no sizeable Doppler shift since the calculated lifetime  $\tau \approx 30$  ps [ref. 7)] exceeds the stopping time for the  $^{93}\text{Tc}$  recoils ( $E \leq 80$  MeV) by more than a factor of 8. Fitting the peaks in the prompt and delayed spectra to Gaussian lineshapes we obtain  $\Delta = E_x(\frac{17}{2}^-) - E_x(\frac{17}{2}^+) = 0.30 \pm 0.03$  keV. This value is in good agreement with the recent measurement by Brown *et al.* 8) using the  $^{92}\text{Mo}(\alpha, p2n)$  reaction ( $\Delta = 0.32 \pm 0.03$  keV) but disagrees with an earlier measurement 7) using the  $^{90}\text{Zr}(\text{Li}, 3n)$  reaction ( $\Delta = 0.44 \pm 0.02$  keV). In the following a value  $\Delta = 0.31 \pm 0.02$  keV is adopted.

In fig. 5 the difference of the centroid energies between the single 756.23 keV  $^{94}\text{Ru}$  transition and the composite  $^{93}\text{Tc}$  transition observed in the delayed spectra (see fig. 1) are shown versus the detector angle. The data are best fitted with a contribution from the  $\frac{17}{2}^- \rightarrow \frac{17}{2}^+ \rightarrow \frac{13}{2}^+$  branch of  $(3 \pm 3\%)$  (solid line in fig. 5). The upper limit on the E1 branch of 6%, together with a calculated conversion coefficient 8,17) of  $8.9 \times 10^3$ , and the lifetime and branching ratios of the  $\frac{17}{2}^-$  state, implies an upper limit  $B(\text{E1}, \frac{17}{2}^- \rightarrow \frac{17}{2}^+) \leq 2.4 \times 10^{-6} e^2 \cdot \text{fm}^2$ .

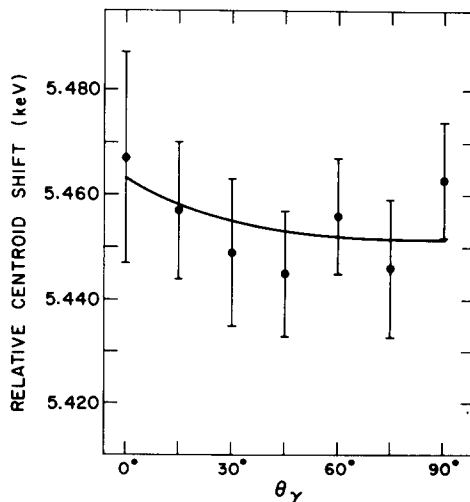


Fig. 5. Centroid of the delayed, composite  $\frac{17}{2}^- \rightarrow \frac{13}{2}^+$  750.78 keV and  $\frac{17}{2}^+ \rightarrow \frac{13}{2}^+$  750.47 keV  $\gamma$ -transition relative to the single 756.23 keV  $\gamma$ -ray in  $^{94}\text{Ru}$ . The solid line indicates that  $\Gamma(\frac{17}{2}^- \rightarrow \frac{17}{2}^+) / \Gamma(\frac{17}{2}^- \rightarrow \frac{13}{2}^+) = (3 \pm 3)\%$ .

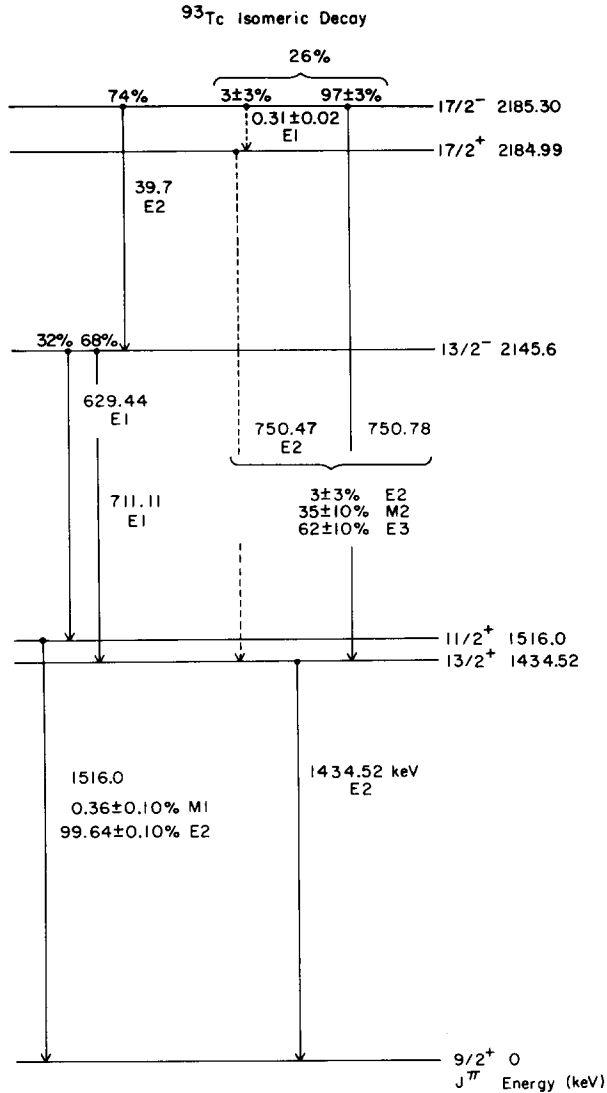


Fig. 6. Decay scheme for the  $^{93}\text{Tc}$   $17/2^-$  isomer determined from the present work (and also from refs. <sup>7-9</sup>). The dashed lines indicate transitions for which only upper limits on the  $\gamma$ -ray intensities have been established.

The present limit is of the same order of magnitude, but on the small side, if compared to other known E1 strengths in  $N = 50$  nuclei <sup>8</sup>).

Because of the similarity of the upper limits on the  $17/2^- \rightarrow 17/2^+$  E1 transition and on the E2 component in the composite 751 keV transition (sect. 5) the already quoted limit of 6% on a p.v.  $\tilde{E}2$  component in the  $17/2^- \rightarrow 13/2^+$  transition cannot be reduced further. A summary of the results from the present work is shown in fig. 6.

### 7. Discussion

Since the  $\frac{17}{2}^- \rightarrow \frac{13}{2}^+$   $\widetilde{E2}$  strength is small the matrix element can be calculated in perturbation theory by summing over all states which are admixed by the p.v. interaction  $H_{p.v.}$ :

$$\begin{aligned} \langle \frac{13}{2}^+ || \widetilde{E2} || \frac{17}{2}^- \rangle &= \sum_i \langle \frac{13}{2}^+ || E2 || \frac{17}{2}^+ i \rangle \langle \frac{17}{2}^+ i | H_{p.v.} | \frac{17}{2}^- \rangle / \Delta E(\frac{17}{2}^-, \frac{17}{2}^+ i) \\ &+ \sum_i \langle \frac{13}{2}^+ | H_{p.v.} | \frac{13}{2}^- i \rangle \langle \frac{13}{2}^- i || E2 || \frac{17}{2}^- \rangle / \Delta E(\frac{13}{2}^- i, \frac{13}{2}^+). \end{aligned} \quad (1)$$

Because of the small energy denominator of 0.3 keV between the first  $\frac{17}{2}^-$  and  $\frac{17}{2}^+$  states, this term dominates (this is the most attractive feature of this case) and hence the E2 matrix element is directly related to the  $\frac{17}{2}^+ \rightarrow \frac{13}{2}^+$  E2 matrix element.

In order to determine  $\langle H_{p.v.} \rangle$  it is simplest to rewrite eq. (1) in terms of the total lifetimes and ratios of partial widths:

$$\langle \frac{17}{2}^+ | H_{p.v.} | \frac{17}{2}^- \rangle = \Delta E \left[ \frac{\tau(\frac{17}{2}^+) \Gamma(\frac{17}{2}^- \rightarrow \frac{13}{2}^+) \Gamma(\widetilde{E2}, \frac{17}{2}^- \rightarrow \frac{13}{2}^+)}{\tau(\frac{17}{2}^-) \Gamma(\frac{17}{2}^-) \Gamma(\frac{17}{2}^- \rightarrow \frac{13}{2}^+)} \right]^{\frac{1}{2}}. \quad (2)$$

All of these are measured quantities except for the  $\frac{17}{2}^+$  lifetime for which we use a value of  $\tau(\frac{17}{2}^+) = 30$  ps based on a calculation <sup>7)</sup> of the  $\langle \frac{13}{2}^+ || E2 || \frac{17}{2}^+ \rangle$  matrix element assuming the well established  $g_{\frac{3}{2}}^n$  shell-model configurations for these states together with a proton effective charge of  $e_p = 1.69e$  deduced from the experimental  $\frac{21}{2}^+ \rightarrow \frac{17}{2}^+$  E2 strength. For  $\Delta E$  we use a value of  $0.31 \pm 0.02$  keV based on the average of the present measurement ( $\Delta E = 0.30 \pm 0.03$  keV) and a previous measurement <sup>8)</sup> ( $\Delta E = 0.32 \pm 0.03$  keV). From previous experiments,  $\tau(\frac{17}{2}^-) = 14.6 \pm 0.4$   $\mu$ s (ref. <sup>9)</sup>),  $\Gamma(\frac{17}{2}^- \rightarrow \frac{13}{2}^+) / \Gamma(\frac{17}{2}^-) = 0.263 \pm 0.010$  (ref. <sup>7)</sup>), and from the present experiment  $\Gamma(\widetilde{E2}; \frac{17}{2}^- \rightarrow \frac{13}{2}^+) / \Gamma(\frac{17}{2}^- \rightarrow \frac{13}{2}^+) \leq 0.064$ . Thus,

$$|\langle \frac{17}{2}^+ | H_{p.v.} | \frac{17}{2}^- \rangle| \leq 0.06 \text{ eV}. \quad (3)$$

This result can be compared to the values of  $|\langle H_{p.v.} \rangle| = 1.2 \pm 0.6$  eV for  $^{19}\text{F}$  and  $|\langle H_{p.v.} \rangle| = 1.2 \pm 0.2$   $\mu$ eV for  $^{180}\text{Hf}$  deduced by assuming mixing between the lowest  $J = \frac{1}{2}$  and  $J = 8$  levels, respectively <sup>4, 6, 8)</sup>.  $H_{p.v.}$  like the normal strong nucleon-nucleon interaction is due to meson exchange and is thus short range. The largest p.v. matrix elements are those between the relative 1s and 1p states. Since the  $^{19}\text{F}$  wave functions are dominated by  $1p_{\frac{1}{2}}$  and  $2s_{\frac{1}{2}}$  valence configurations, it can be expected to have one of the largest possible p.v. matrix elements.

The dominant configurations for  $^{93}\text{Tc}$  are  $|(g_{\frac{3}{2}})^4(2p_{\frac{1}{2}})^{\frac{17}{2}^-} \rangle$  and  $|(1g_{\frac{3}{2}})^3(2p_{\frac{1}{2}})^2 \frac{17}{2}^+ \rangle$  and the p.v. matrix element is proportional to

$$\langle \frac{17}{2}^+ | H_{p.v.} | \frac{17}{2}^- \rangle \approx \langle g_{\frac{3}{2}}^2 4^+ | H_{p.v.} | g_{\frac{3}{2}} p_{\frac{1}{2}} 4^- \rangle. \quad (4)$$

Unfortunately, this does not have a large overlap comparable with the  $\langle 2s | H_{p.v.} | 1p \rangle$  relative matrix element. It may thus not be surprising that the present limit in  $^{93}\text{Tc}$  is much smaller than the matrix element in  $^{19}\text{F}$ , but detailed calculations remain to

be carried out. The <sup>93</sup>Tc p.v. matrix element may be enhanced by admixtures outside the  $g_{3/2}$ - $p_{1/2}$  model space; in fact such admixtures are required to explain the observed E1 strengths<sup>8)</sup> for the  $N = 50$  nuclei.

Finally, we note that the very small p.v. matrix element in <sup>180</sup>Hf is due to the large change ( $\Delta K = 8$ ) in intrinsic structure for the  $8^-$  and  $8^+$  states. As observed in ref.<sup>8)</sup> the scaling relation

$$\frac{|\langle J^+ | H_{p.v.} | J^- \rangle|}{[B(E1; J^- \rightarrow J^+)]^{1/2}} \approx 100 \text{ eV} \cdot e^{-1} \cdot \text{fm}^{-1}$$

connects the experimental matrix elements in <sup>19</sup>F and <sup>180</sup>Hf. This relation is consistent with the present results in <sup>93</sup>Tc but it is not very useful since only an upper limit is obtained for the  $\frac{17^-}{2} \rightarrow \frac{17^+}{2}$  transition,  $B(E1) \leq 2.4 \times 10^{-6} e^2 \cdot \text{fm}^2$ .

In order to reduce the experimental limit on the  $\widetilde{E2}$  strength, the  $\widetilde{E2}$ -M2 interference term should be measured by observing the  $\gamma$ -ray asymmetry of a polarized state or by observing  $\gamma$ -ray circular polarization. The  $\gamma$ -ray circular polarization  $P_\gamma$  and the  $\gamma$ -ray asymmetry  $A_K$  (ref.<sup>4)</sup>) are given (neglecting terms of the order  $\varepsilon^2$ ) by

$$P_\gamma = \frac{2\varepsilon}{1+\delta^2} = (0.72^{+0.12}_{-0.20})\varepsilon,$$

$$A_K = \frac{2\varepsilon}{1+\delta^2} [F_K(2, 2, \frac{17}{2}, \frac{13}{2}) + \delta F_K(2, 3, \frac{17}{2}, \frac{13}{2})],$$

$$A_1 = \frac{2\varepsilon}{1+\delta^2} [-0.6104 - 0.5397\delta] = -(1.0 \pm 0.3)\varepsilon,$$

$$A_3 = \frac{2\varepsilon}{1+\delta^2} [0.5286 + 0.2727\delta] = 0.64 \pm 0.20)\varepsilon,$$

where  $\delta$  is the E3/M2 mixing ratio and  $\varepsilon$  is the  $\widetilde{E2}$ /M2 mixing ratio as defined in ref.<sup>15)</sup>, and the  $F$ -coefficients are defined in ref.<sup>18)</sup>. Using the present experimental value of  $|\varepsilon| \leq 0.5$ , we obtain  $|P_\gamma| \leq 0.42$  and  $|A_1| \leq 0.65$ . Thus these effects may be very large compared to other cases [e.g.,  $|\varepsilon| = 0.038 \pm 0.004$  for the  $8^- \rightarrow 6^+$  transition in <sup>180</sup>Hf (ref.<sup>4)</sup>).

However, these measurements would not be easy. Since the isomer can only be populated in evaporation reactions [e.g. (p, 2n), (<sup>6</sup>Li, 3n)], it seems unlikely that a large polarization would be transferred in the reaction and it would be difficult to calculate the polarization transfer. The  $\gamma$ -ray circular polarization measurements are difficult because the detection efficiency is low (1%–2%). Before these experiments are carried out, it would seem important to have a theoretical estimate of the p.v. matrix element, since they would be especially difficult if  $\varepsilon$  is much less than the present experimental upper limit.

The future role of <sup>93</sup>Tc in understanding parity violation does not appear especially promising. The main reason for this is that the experimental <sup>93</sup>Tc p.v. matrix element



turns out to be “hindered” relative to the p.v. matrix element in  $^{19}\text{F}$ . As a next step, a calculation of the  $^{93}\text{Tc}$  matrix element and a comparison with the presently established limit would seem worthwhile.

### References

- 1) S. Weinberg, *Rev. Mod. Phys.* **46** (1974) 255
- 2) M. Gari, *Phys. Reports* **6C** (1973) 319;  
M. A. Box, B. H. McKellar, P. Pick and K. R. Lassey, *J. of Phys.* **G1** (1975) 493
- 3) M. Gari, in *Interaction studies in nuclei*, ed. A. Jochim and B. Ziegler (North-Holland, Amsterdam, 1975) p. 307;  
B. Desplanques and J. Micheli, *Phys. Lett.* **68B** (1977) 339
- 4) K. S. Krane, C. E. Olsen, J. R. Sites and W. A. Steyert, *Phys. Rev.* **C4** (1971) 1906;  
K. S. Krane, C. E. Olsen and W. A. Steyert, *Phys. Rev.* **C5** (1972) 1663
- 5) C. A. Barnes, M. M. Lowry, J. M. Davidson, R. E. Marrs, F. B. Morinigo, B. Chang, E. G. Adelberger and H. E. Swanson, *Phys. Rev. Lett.* **40** (1978) 840
- 6) E. G. Adelberger, H. E. Swanson, M. D. Cooper, J. W. Tape and T. A. Trainor, *Phys. Rev. Lett.* **34** (1975) 402;  
E. G. Adelberger, H. E. Swanson and T. A. Trainor, *Univ. of Washington at Seattle Annual Report 1976*, p. 58
- 7) B. A. Brown, D. B. Fossan, P. M. S. Lesser and A. R. Poletti, *Phys. Rev.* **C13** (1976) 1194
- 8) B. A. Brown, R. A. Warner, L. E. Young and F. M. Bernthal, *Phys. Rev.*, to be published
- 9) O. Häusser, I. S. Towner, T. Faestermann, H. R. Andrews, J. R. Beene, D. Horn, D. Ward and C. Broude, *Nucl. Phys.* **A293** (1977) 248
- 10) G. B. Hagemann, R. Broda, B. Herskind, H. Ishihara, S. Ogaza and H. Ryde, *Nucl. Phys.* **A245** (1975) 166;  
J. R. Beene, O. Häusser, A. J. Ferguson, H. R. Andrews, M. A. Lone, B. Herskind and C. Broude, to be published
- 11) R. S. Simon, M. V. Banaschik, R. M. Diamond, J. O. Newton and F. S. Stephens, *Nucl. Phys.* **A290** (1977) 253
- 12) F. A. Rossini and W. D. Knight, *Phys. Rev.* **178** (1969) 641
- 13) P. A. Butler, P. E. Carr, L. L. Gadeken, A. N. James, P. J. Nolan, J. F. Sharpey-Schafer, P. J. Twin and D. A. Viggars, *Nucl. Instr.* **108** (1973) 497
- 14) K. Alder, A. Bohr, T. Huus, B. Mottelson and A. Winther, *Rev. Mod. Phys.* **28** (1956) 432
- 15) H. J. Rose and D. M. Brink, *Rev. Mod. Phys.* **39** (1967) 306
- 16) P. Taras, *Can. J. Phys.* **49** (1971) 328
- 17) H. C. Pauli and U. Raff, *Computer Phys. Comm.* **9** (1975) 392
- 18) T. Yamazaki, *Nucl. Data* **A3** (1967) 1